Characterization of a Balanced Homodyne Detection for Optical Explanations

Alejandro Guerrero Pantoja*
Universidad de los Andes, Bogotá, Colombia.
(Dated: 3 de junio de 2024)

In the realm of quantum optics, the precise characterization of various noise sources such as shot noise, electric noise, and vacuum noise is pivotal for advancing optical measurement technologies and quantum information systems. This study introduces an experimental approach using homodyne detection to convert fluctuations in light intensity into voltage signals. These signals are then analyzed with the aid of an oscilloscope or a spectrum analyzer to dissect the temporal and spectral characteristics of the noise. The integration of these tools allows for a detailed observation and differentiation of quantum noises, providing insights that are critical for refining the accuracy and efficiency of optical systems. This project was primarily based on two parts: optics and electronics, we successfully completed the optical part, while the electrical component remains for future investigation. These findings lay the groundwork for improved quantum noise characterization, enhancing the development of next-generation optical and quantum information technologies.

I. INTRODUCTION

In the rapidly evolving field of quantum optics, the precise characterization of noise is fundamental to the advancement of optical measurement technologies and quantum information systems. Noise sources such as shot noise, electrical noise, and vacuum noise pose significant challenges, necessitating sophisticated techniques for their identification and analysis [1]. Among the various methods available, balanced homodyne detection stands out as a powerful technique for converting fluctuations in light intensity into measurable voltage signals, thereby enabling detailed noise characterization [2].

Balanced homodyne detection leverages the principles of interference to enhance the sensitivity of measurements, making it a crucial tool in quantum optics. This method involves the use of a local oscillator, typically a laser with a well-defined phase, which interferes with the signal beam at a photodetector. The difference in intensity between the two beams is measured, allowing for the precise quantification of noise components [3]. The ability to distinguish between different types of noise, such as quantum noise originating from the intrinsic properties of light and noise from electronic components, is critical for the refinement of optical systems. A key aspect of this study is the application of the Mach-Zehnder interferometer, a device renowned for its high capability in spatial and spectral analysis. By employing a 633 nm Helium-Neon (HeNe) laser beam, the interferometer provides a robust platform for examining the intrinsic characteristics of quantum noise [4].

* Correo institucional: a.guerrerop@uniandes.edu.co

The use of advanced analytical tools, such as oscilloscopes and spectrum analyzers, facilitates a comprehensive examination of the temporal and spectral properties of the noise, offering valuable insights for enhancing the accuracy and efficiency of optical measurements [5].

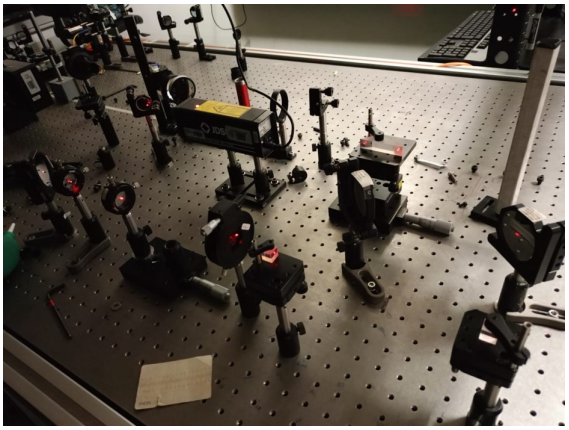

Figura 1. Implementation of the Mach-Zehnder Interferometer on the Optical Table in the Laboratory

This project is structured around two primary components: optics and electronics. The optical component has been successfully completed, demonstrating the effectiveness of the Mach-Zehnder interferometer in noise characterization. The remaining electrical component, which involves further investigation into the noise introduced by electronic devices, presents a promising avenue for future research. By integrating the findings from both components, this study aims to provide a deeper understanding of quantum noise and its impact on optical systems.The insights gained from this research have significant implications for the development of next-generation optical and quantum information technolo-

gies.

II. METHODOLOGY

As previously mentioned, this project is divided into two main components: the optical and electronic components. By combining them, this methodology enables a thorough characterization of noise in the BHD system.

A. Optical Component

This component involves the setup and alignment of the Mach-Zehnder interferometer on the optical table. The setup begins with arranging key optical elements, including beam splitters, mirrors, and the 633 nm Helium-Neon (HeNe) laser, on the optical table, Figure 1. Next, the interferometer's arms are carefully aligned to achieve optimal interference patterns [6], this involves adjusting the position and orientation of the mirrors and beam splitters to ensure that the laser beams recombine at the photodetector with the desired phase relationship [2]. The optical setup is then calibrated using known reference signals to ensure accurate measurement of light intensity fluctuations, verifying the linearity and sensitivity of the detectors [3].

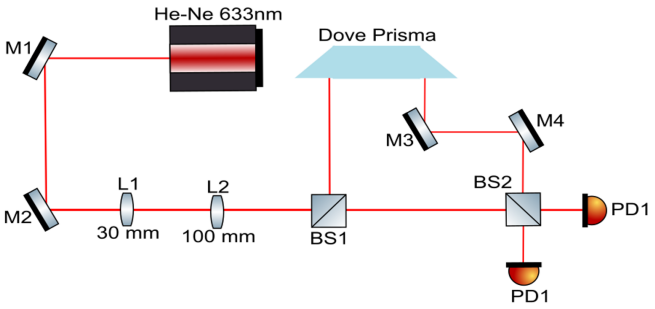

Figura 2. This image illustrates the graphical model of the implemented Mach-Zehnder interferometer. The model includes key components such as beam splitters, mirrors, and detectors. This visual representation aids in understanding the alignment and functioning of the interferometer within the laboratory setup.

B. Electronic Component

The electronic component, specifically the design and implementation of the transimpedance circuit, has not been completed due to time constraints. But we must say that the transimpedance circuit is crucial for converting the photocurrent into a measurable voltage signal with enhanced sensitivity and accuracy, although this part of the project is designated for future work. The design of the transimpedance amplifier circuit involves selecting appropriate operational amplifiers, feedback resistors, and other components to achieve the desired gain and bandwidth [7]. Constructing this circuit on a breadboard or printed circuit board (PCB) with attention to minimizing noise and interference is a critical step that will be undertaken in subsequent phases of the project.

Without the transimpedance circuit, the photodiodes are directly connected to the oscilloscope or spectrum analyzer. This direct connection limits the sensitivity and accuracy of the noise measurements due to the lower signal-to-noise ratio and the potential for electronic noise interference [8]. As a result, the data collected in the current setup may not fully capture the finer details of the noise characteristics, such as shot noise and quantum noise, which are essential for precise noise characterization [1]. This enhancement will allow for more accurate and sensitive measurements of noise, providing a clearer distinction between different noise sources [9]. The improved data quality will facilitate a deeper understanding of the intrinsic noise characteristics of the optical system and the electronic components [10].

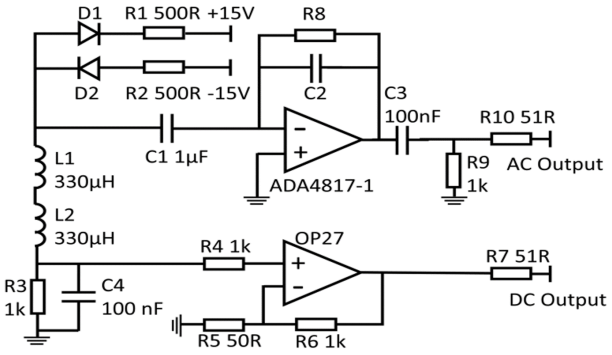

Figura 3. Here we illustrate the model of the transimpedance circuit used in the balanced homodyne detector (BHD). The model shows the configuration of the photodetector, operational amplifier, and feedback resistor, which are essential for converting the photocurrent into a measurable voltage signal. This circuit is crucial for enhancing the sensitivity and accuracy of noise measurements in the optical detection system. Emphasize that the model was selected and adapted to meet our requirements from [9]

III. RESULTS AND DISCUSSION

Here we present the experimental results obtained from the BHD system for optical measurements. The key parameters measured include the Rayleigh range

z_R, the position of the beam waist z_0, the minimum beam waist ω_0, and the visibility V.

$$\omega(z) = \omega_0 \sqrt{1 + \left(\frac{z - z_0}{z_R}\right)^2} \quad where \quad z_R = \frac{\pi \omega_0^2}{\lambda} \quad (1)$$

Equations describing the beam waist of a Gaussian beam, Where the variable $\omega(z)$ represents the beam radius at position z, ω_0 is the minimum beam waist, z_0 is the position of the beam waist, z_R is the Rayleigh range, and λ is the wavelength of the laser.

The minimum beam waist ω_0 was found to be $1677{,}64 \pm 16{,}79 \mu m$ Equation 1. This parameter is essential for characterizing the focusing properties of the laser beam and understanding the beam's spatial profile. The fit used to determine ω_0 is shown in Figure 4. The Rayleigh range z_R was measured to be $3{,}48 \pm 0{,}04 m$ Equation 1. This parameter is crucial as it indicates the distance over which the beam radius increases by a factor of $\sqrt{2}$, reflecting the divergence of the beam. The position of the beam waist z_0 was determined to be $0{,}613 \pm 0{,}002$ centimeters Equation 1, representing the location along the beam propagation axis where the beam radius is at its minimum.

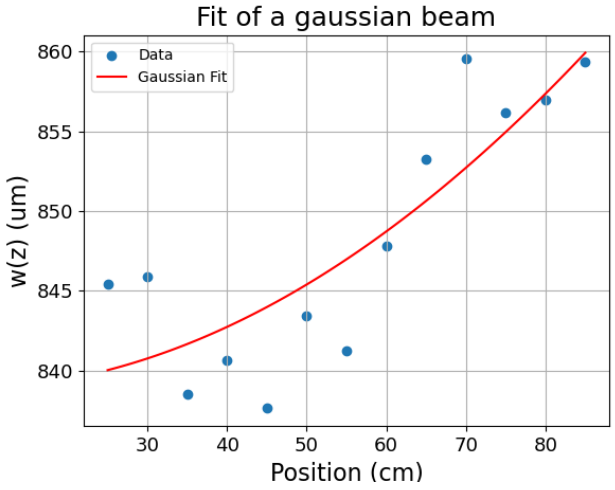

Figura 4. Fitting the beam waist of the laser. The graph shows the experimental data of the laser beam waist measurements along with the fitted curve. From this fit, the beam parameters were determined: the Rayleigh range (Z_r), the beam waist location (Z_0), and the minimum beam waist (W_0). These parameters are crucial for characterizing the Gaussian beam profile and understanding the propagation characteristics of the laser used in the experiment.

$$P = P_m \left(1 \pm V \cos\left(\frac{2\pi \Delta x}{\lambda}\right)\right) \quad (2)$$

$$P_m = \frac{P_{max} + P_{min}}{2} \quad (3)$$

Equations describing the average power and modulated power of an interferometric signal, where the variable P_m represents the average power, calculated as the mean of the maximum power P_{max} and the minimum power P_{min}. The variable P represents the power at a given position Δx, where V is the visibility of the interference pattern, and λ is the wavelength of the light.

The theoretical behavior of the Mach-Zehnder interferometer was analyzed to understand the expected interference patterns. The theoretical graph, which plots the power in each arm of the interferometer as a function of displacement, is shown in Figure 5. This analysis helps in predicting the interference behavior under ideal conditions.

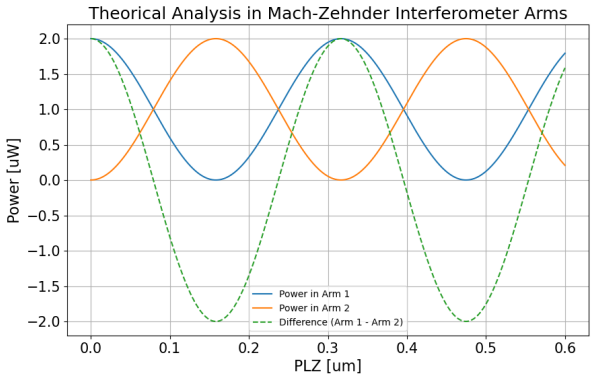

Figura 5. The plot displays the power in each arm of the interferometer (Arm 1 and Arm 2) as a function of displacement in micrometers. The difference in power between the two arms (Arm 1 - Arm 2) is also shown, highlighting the interference pattern resulting from the superposition of light waves. This graph was generated using Python and the "matplotlib"library, with the code calculating the phase shift and resulting intensities based on the displacement and wavelength.

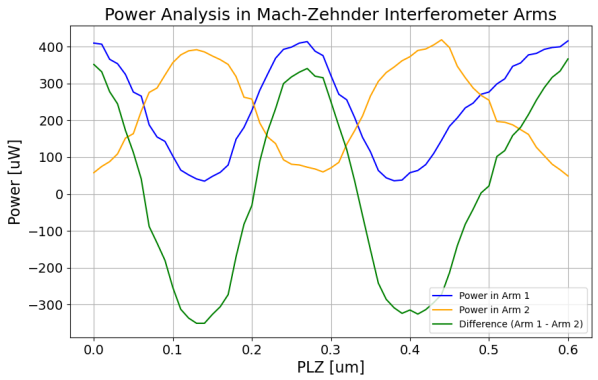

Figura 6. The plot illustrates experimental measurements of the recorded power levels in both arms of the interferometer (Arm 1 and Arm 2) as displacement in micrometers varies. The difference in power between the two arms (Arm 1 - Arm 2) is also depicted, showcasing the interference pattern due to light wave superposition. This data, obtained from actual experimental setup, was processed and visualized using Python and the 'matplotlib' library.

$$V = \frac{P_{max} - P_{min}}{P_{max} + P_{min}} \tag{4}$$

Equation for calculating the visibility V of an interference pattern. V is a measure of the contrast between the maximum power P_{max} and the minimum power P_{min} of the interference fringes. It is calculated as the difference between the maximum and minimum power divided by their sum, indicating the degree of modulation in the interference signal. The visibility V of the interference pattern was calculated to be $0{,}876 \pm 0{,}005$, indicating a high degree of modulation. The experimental behaviour are presented in Figure 6.

IV. CONCLUSIONS

This study has explored the implementation and characterization of a balanced homodyne detection system for optical measurements, emphasizing the significance of precise noise characterization in advancing quantum optics and optical measurement technologies.

The successful setup and alignment of the Mach-Zehnder interferometer on the optical table demonstrated the effectiveness of the system in converting light intensity fluctuations into measurable voltage signals. Through careful calibration and data collection, we were able to analyze the temporal and spectral characteristics of the beam. The experimental findings confirmed the theoretical predictions of the Mach-Zehnder interferometer's behavior, providing valuable insights into the interference patterns. The visibility measurements and their uncertainties were calculated, demonstrating the system's capability to perform precise optical measurements.

Future work will focus on completing the electronic component, specifically the transimpedance circuit, and further refining the measurement setup to reduce uncertainties and enhance overall system performance. The future implementation of the transimpedance circuit is expected to significantly enhance the sensitivity and accuracy of noise measurements by amplifying the photocurrent and reducing electronic noise. This enhancement will provide a clearer distinction between different noise sources, leading to improved data quality and a deeper understanding of the intrinsic noise characteristics of the optical system and electronic components.

[1] H.-A. Bachor and T. C. Ralph, *A guide to experiments in quantum optics*. John Wiley & Sons, 2004.
[2] A. I. Lvovsky and M. G. Raymer, "Continuous-variable optical quantum-state tomography," *Reviews of Modern Physics*, vol. 81, no. 1, p. 299, 2009.
[3] D. F. Walls and G. J. Milburn, *Quantum optics*. Springer Science & Business Media, 2008.
[4] V. B. Braginsky and F. Y. Khalili, *Quantum measurement*. Cambridge University Press, 1992.
[5] C. M. Caves, "Quantum-mechanical noise in an interferometer," *Physical Review D*, vol. 23, no. 8, p. 1693, 1981.
[6] A. M. Silva and Valencia, "Characterization of quantum states of light by means of homodyne detection and reconstruction of wigner functions," *Monografia Uniandes*.
[7] P. Horowitz and W. Hill, *The art of electronics*. Cambridge University Press, 2015.
[8] M. C. W. Rossum and T. M. Nieuwenhuizen, "Response of the modulation transfer function to noise," *Reviews of Modern Physics*, vol. 71, no. 1, p. 313, 1997.
[9] S. Lang, S. Zhang, X. Li, Y. Niu, and S. Gong, "Low noise balanced homodyne detector for quantum noise measurement," vol. 10, pp. 27912–27916.
[10] X. Zhang, Y.-C. Zhang, Z. Li, S. Yu, and H. Guo, "1.2 GHz balanced homodyne detector for continuous-variable quantum information technology," vol. 10, no. 5, pp. 1–10.

Apéndice A: Error Analysis

1. Standard Deviation and Uncertainty

The standard deviation (σ) of a set of measurements is a measure of the dispersion or spread of the data points. It is calculated as follows:

$$\sigma = \sqrt{\frac{1}{N-1}\sum_{i=1}^{N}(x_i - \bar{x})^2} \tag{A1}$$

where N is the total number of measurements, x_i is each individual measurement and $\bar{x}$ is the average value of the measurements.

2. Uncertainty Propagation

When combining multiple measurements, the uncertainty propagation formula is used to determine the combined uncertainty. For a function $f(x_1, x_2, \ldots, x_n)$ with variables x_i and their uncertainties σ_{x_i}, the combined uncertainty σ_f is given by:

$$\sigma_f = \sqrt{\left(\frac{\partial f}{\partial x_1}\sigma_{x_1}\right)^2 + \left(\frac{\partial f}{\partial x_2}\sigma_{x_2}\right)^2 + \cdots + \left(\frac{\partial f}{\partial x_n}\sigma_{x_n}\right)^2} \tag{A2}$$

This formula allows for the calculation of the overall uncertainty of a result that depends on multiple measured values, each with their own uncertainties.

3. Visibility Calculation

To calculate the visibility (V) of the beam, we use the Equation 4. So, having the maximum value $P_{\max} = 416{,}3\,\mu W$ and the minimum value $P_{\min} = 27{,}4\,\mu W$, we calculate the visibility as $V \approx 0{,}8765$. To determine the uncertainty in the visibility, we assume a relative uncertainty for both $P_{\max}$ and $P_{\min}$. The standard deviations are:

$$s_{\max} = 0{,}01 \times 416{,}3\,\mu W = 4{,}163\,\mu W \tag{A3}$$

$$s_{\min} = 0{,}01 \times 27{,}4\,\mu W = 0{,}274\,\mu W \tag{A4}$$

The standard error of the mean for each value is:

$$\sigma_{P_{\max}} = \frac{s_{\max}}{\sqrt{3}} = \frac{4{,}163}{\sqrt{3}} \approx 2{,}40\,\mu W \tag{A5}$$

$$\sigma_{P_{\min}} = \frac{s_{\min}}{\sqrt{3}} = \frac{0{,}274}{\sqrt{3}} \approx 0{,}158\,\mu W \tag{A6}$$

Using the error propagation formula for visibility:

$$\sigma_V = V\sqrt{\left(\frac{\sigma_{P_{\max}}}{P_{\max} - P_{\min}}\right)^2 + \left(\frac{\sigma_{P_{\min}}}{P_{\max} + P_{\min}}\right)^2} \tag{A7}$$

Thus, the visibility and its uncertainty are:

$$V = 0{,}876 \pm 0{,}005 \tag{A8}$$

4. Impact of Sensitivity on Measurements

The sensitivity of the experimental detectors or components can significantly affect the measurements. High sensitivity can lead to smaller uncertainties, resulting in more accurate and reliable data. Conversely, lower sensitivity can increase the uncertainties, thereby affecting the precision of the results. It is crucial to calibrate and maintain the sensitivity of the equipment to ensure the accuracy of the measurements.